ENVIRONMENTAL RESEARCH
LETTERS

OPEN ACCESS

RECEIVED
8 February 2024

REVISED
24 May 2024

ACCEPTED FOR PUBLICATION
10 June 2024

PUBLISHED
21 June 2024

LETTER

Nexus between the deficit in moisture transport and drought occurrence in regions with projected drought trends

Luis Gimeno-Sotelo[1,*], **Milica Stojanovic**[1], **Rogert Sorí**[1], **Raquel Nieto**[1], **Sergio M Vicente-Serrano**[2] and **Luis Gimeno**[1]

[1] Centro de Investigación Mariña, Universidade de Vigo, Environmental Physics Laboratory (EPhysLab), Ourense, Spain
[2] Instituto Pirenaico de Ecología, Consejo Superior de Investigaciones Científicas (IPE–CSIC), Zaragoza, Spain
[*] Author to whom any correspondence should be addressed.

E-mail: luis.gimeno-sotelo@uvigo.es

Keywords: meteorological drought, moisture transport, moisture sources, FLEXPART, copulas

Supplementary material for this article is available online

Abstract

In this article, we focus on studying the nexus between moisture transport deficit and drought occurrence in nine key regions across the world where the magnitude of meteorological drought is projected to increase from 1850 to 2100 under a high anthropogenic emission scenario. These regions are central America, southwestern South America, northern Brazil, the Amazon, northeastern Brazil, the western Mediterranean, southern Africa, the eastern Mediterranean, and southwestern Australia. Using the Lagrangian particle dispersion model FLEXPART, we identify the specific moisture sources of the regions (the own region, the nearby continental source and the oceanic sources) and obtain their contributions to the precipitation in the regions for the period 1980–2018. For each region and specific moisture source, the conditional probability of meteorological drought occurrence given an equivalent contribution deficit from the source is estimated using copula models, a statistical methodology that allows us to capture complex relationships between variables. We identify the dominant moisture source in each region, which is the source for which the contribution deficit maximises drought probability. A variety of cases are found: in three regions, the dominant source is the region itself, in one region, it is the nearby terrestrial source, and in five regions, it is an oceanic source. In general, contribution deficits from specific moisture sources are associated with only slightly greater drought probabilities than those from major global moisture sources. We also reveal that the source that contributes the most to precipitation in a given region is not necessarily the dominant source of drought in the region. These results highlight the importance of understanding the role of dominant moisture sources and moisture transport deficits on meteorological drought occurrence at a regional scale.

1. Introduction

Drought is one of the main natural hazards at the global level and strongly impacts ecosystems and society through significant economic losses that lead to far-reaching humanitarian disasters (Erian *et al* 2021, IPCC 2022). To illustrate this in an easy-to-interpret-way, drought accounts for annual economic losses in the United States of America of approximately $6.4 billion (NOAA-NCEI 2021) and €9 billion in the European Union (Cammalleri *et al* 2020, Naumann *et al* 2021). Although drought is a recurrent phenomenon that occurs in every region as a consequence of natural climate variability (Stine 1994, Woxodhouse *et al* 2010), the last IPCC report (Seneviratne *et al* 2021) concluded that there is medium confidence that climate change is responsible for the occurrence of more severe meteorological droughts in some regions of the world. Moreover, there is high confidence that more frequent and severe meteorological droughts will be recorded in some regions of the world under high global warming scenarios (Seneviratne *et al* 2021).

Despite the uncertainties associated with future emission scenarios, climate models, and the definition of drought, the use of multiple climate models

together with multiple ways of identifying droughts allows us to find regions where there is greater agreement between models on the intensification of meteorological drought with climate change. Projections based on high warming scenarios in CMIP5 and CMIP6 show more frequent and severe droughts over great extensions of the world including in most of them southern North America, Central America, the Amazon region, the Mediterranean region, southern Africa, and southern Australia. The high agreement in the projections of different Earth System Models suggests that in these regions, there is high confidence that meteorological drought will intensify, particularly under high global warming scenarios.

Although drought has a multidimensional aspect and depends on different processes and interactions (Douville *et al* 2021), leading to different drought types and associated impacts (agricultural, hydrological and socioeconomic) (Wilhite *et al* 2007, Bachmair *et al* 2015), the main variable defining drought severity is indisputably the occurrence of a precipitation deficit relative to the mean climate. The dynamic and thermodynamic mechanisms that cause precipitation deficits are very complex, but to put it simply, precipitation depends on whether there is moisture in the air and whether it is forced to rise. With respect to moisture, the moisture contained in the atmospheric column at any given time is usually insufficient to produce the precipitation recorded at that location (Trenberth *et al* 2003), and deficiencies in moisture transport are essential to explain precipitation deficits (Gimeno *et al* 2012, 2016, Drumond *et al* 2019).

There is a series of published studies on moisture transport deficits and drought occurrence at the regional level based on different techniques, including sophisticated Lagrangian or semi-Lagrangian techniques, which can be used to accurately locate the main moisture sources responsible for precipitation in a region (see e.g. Salah *et al* 2018, Garcia-Herrera *et al* 2019, Herrera-Estrada *et al* 2019, Roy *et al* 2019, Wei and Dirmeyer 2019, Holgate *et al* 2020, Schumacher *et al* 2022). These works have been carried out for the present climate, given the enormous technical difficulties and the need for very intensive computations derived from using Lagrangian techniques in climate models. However, even when analysed in the present climate, these works are of interest in regions where changes are projected for the future since they locate the source regions where climate models should be focused, dealing with aspects such as the intensity of the source (evaporation–precipitation balance) or the source–sink circulation.

Recently, Gimeno-Sotelo *et al* (2024b) demonstrated that meteorological droughts are strongly connected with moisture transport deficits from major global moisture sources. Given the relevance of the processes driving drought severity, with implications for future climate scenarios, the main objectives of this work are (i) to analyse whether, given a moisture transport deficit, the probability of drought occurrence notably changes if, instead of using major global moisture sources, the specific moisture sources of the region are used and (ii) to determine whether the specific moisture source that most contributes to precipitation in a region is the dominant source for drought occurrence. Since these objectives essentially involve regional analyses, we are forced to choose a finite number of study regions. In this article, because of the relevance of drought to climate change, we focused on regions where there is the greatest confidence in drought intensification with global warming and where understanding drought mechanisms is a priority.

2. Materials and methods

2.1. Identification of key regions

To identify the regions in which increases in meteorological drought severity are projected, we used monthly precipitation data for the historical period (1850–2014) and the Shared Socioeconomic Pathway 5–8.5 (SSP5-8.5) from 2015 to 2100. These data were obtained from an ensemble of 18 CMIP6 models (Eyring *et al* 2016), namely, ACCESS-CM2, ACCESS-ESM1-5, CanESM5-CanOE, CanESM5, CMCC-ESM2, CNRM-CM6-1-HR, CNRM-CM6-1, CNRM-ESM2-1, FIO-ESM-2-0, GFDL-ESM4, GISS-E2-1-G, HadGEM3-GC31-LL, HadGEM3-GC31-MM, INM-CM4-8, IPSL-CM6A-LR, MIROC-ES2L, MIROC6, MRI-ESM2-0, and interpolated to a common resolution of 2.5° × 2.5° using bilinear transformation. As in Gimeno-Sotelo *et al* (2024a), the analysis consisted of applying the run theory (Tallaksen *et al* 1997, Fleig *et al* 2006) to identify drought events. Trends were obtained by fitting a linear regression model to the annual series of magnitude values of drought events as a function of time, and significance was assessed using the Mann–Kendall test (1945, 1948) at a significance level of 0.05. The selection of key regions was based on high model agreement (at least 90%) in terms of a significant increase in the magnitude of drought events from 1850 to 2100.

The unfavourable SSP5-8.5 scenario was used because of the large socio-economic impacts that it may imply. The selection of other more favourable SSPs would not add more information to this paper than the analysis of different regions, most of which are similar to those in the SSP5-8.5, as is the case for North America, Central America, the Mediterranean, the Amazon, or southwestern Australia, where the difference is the severity of drought in the lower warming scenarios, which is significantly reduced (Cook *et al* 2020).

2.2. Identification of specific moisture sources in each region

The Lagrangian particle dispersion model FLEXPART v9.0 (Stohl *et al* 2005, Pisso *et al* 2019) was used to determine the sources and sinks of moisture by tracking water vapour trajectories. FLEXPART was constrained by 6-h specific humidity and 3D-wind data, among other data also used for internal model parameterisations (Pisso *et al* 2019), taken from the whole available period (1980–2018) of the ERA-Interim reanalysis (Dee *et al* 2011) from the European Centre for Medium-Range Weather Forecasts (ECMWF) at a 1° horizontal resolution (regridded from the original reduced Gaussian grid N128) and within 61 vertical levels of the atmosphere. We acknowledge the improvements of the latest ECMWF reanalysis, ERA5 (Hersbach *et al* 2020), over ERA-Interim; however, with these input data, FLEXPART has already been successfully and extensively used to identify the origin of precipitating moisture for different regions and synoptic weather systems (see e.g. Gimeno-Sotelo *et al* 2024b, and the review by Gimeno *et al* 2020). In addition, a recent paper by Fernández-Alvarez *et al* (2023) performed a comparison between the results of FLEXPART forced with ERA-Interim and ERA5 reanalyses and found no significant differences between the moisture source patterns.

The atmosphere was divided into approximately two million air particles that are moved by winds in a 3D space. The method was based on calculating the changes in the specific humidity of all particles (with constant mass, m) at 6 h intervals ($\frac{dq}{dt}$) along their trajectories and aggregating the net increases and decreases in humidity within the vertical atmospheric column over a given surface grid cell (of area A, 0.25° in this study, using linear interpolation; see Nieto and Gimeno 2019 for further details). This enabled the determination of the net flux of fresh water ($E-P=\frac{\sum m\frac{dq}{dt}}{A}$), which is the difference between evaporation (E) and precipitation (P). This approach has been used in several papers to calculate moisture sources and sinks in specific areas or meteorological systems (e.g. Gimeno *et al* 2010a; Algarra *et al* 2020, Vazquez *et al* 2020, Fernández-Alvarez *et al* 2023). A summary of the advantages and disadvantages of the method compared to other approaches for the calculation of moisture sources and sinks can be found in Gimeno *et al* (2012), (2020).

To identify the main specific climatological moisture sources of a given region, global outputs of the FLEXPART model were used for the period 1980–2018. The air masses that reach each independent region were backwards-tracked in time based on the mean optimal residence time of water vapour (Nieto and Gimeno 2019, 2021). Areas where air masses gain moisture along their pathway, i.e. where evaporation exceeds precipitation in the net moisture balance (E-P) > 0), were identified as moisture sources. To delimit the main individual moisture sources for each region, the 90% percentile threshold was applied to the annual climatological positive (E-P) values, encompassing areas where (E-P) is greater than that percentile. This technique has been previously applied for the same purpose in several papers (see Gimeno *et al* 2020).

2.3. Calculation of drought indices and moisture source contribution deficit indices

The standardised precipitation index (SPI) (McKee *et al* 1993) was used for the identification of meteorological droughts. This index was defined in standard deviations and was calculated from monthly precipitation series on different time scales, defined as the cumulative precipitation over a number of n months. The precipitation series accumulated on the chosen time scale was fitted to a gamma distribution according to the WMO recommendation (WMO 2012), and the cumulative probabilities were calculated and transformed into a standard normal distribution. Negative SPI values indicate less than median precipitation and consequently dry conditions, whereas positive values represent the opposite. The standardised nature of the SPI allows comparisons between regions with very different precipitation magnitude and seasonality. For the SPI calculation, the monthly gridded multi-source weighted-ensemble precipitation dataset (MSWEP) (Beck *et al* 2017) with a horizontal resolution of 0.1° was used for the period of 1980–2018.

Once the main moisture sources of each region were defined, to determine their contribution to the precipitation in the target region, the air masses were tracked forward in time. In forward tracking, the areas where the moisture is lost as precipitation are identified where negative values of the net moisture balance ((E-P) < 0) occur, which means where precipitation exceeds evaporation. That is, when there is an aggregated loss in specific humidity for all the air particles departing from the source and reaching each grid cell in the target region. The monthly sum of these negative values over the target region is assumed to indicate the precipitation coming for that month from the source involved in the analysis. The modulus of that quantity is used for practical reasons. Thus, for each region, a time series of the contribution to the precipitation in the region from its specific moisture sources could be constructed, and indices analogous to the

SPI could be computed (these indices are denoted as SPIc).

2.4. Estimation of conditional probabilities through copulas

As in Gimeno-Sotelo *et al* (2024b), we relied on copula models to estimate the conditional probability of drought (SPI lower than a certain threshold) given an equivalent moisture deficit from a source (SPIc lower than the same threshold) because this methodology allowed us to produce large amounts of synthetic data that reproduced the complex relationships between variables. The methodology consisted of transforming the original data to uniform-scale values and applying the maximum likelihood estimation to fit several copula models, namely, the Gaussian, Student-t, Clayton, Gumbel, Frank and Joe copulas (see Czado 2019), which have different features in terms of symmetry/asymmetry and tail dependence. A model was selected according to the Akaike information criterion (1974), and the goodness of fit was assessed by means of a test described by Huang and Prokhorov (2014) based on White´s (1982) information matrix equality. A total of 100 000 simulated values for the variables on a uniform scale were obtained from the selected copula model. Using the simulated values, it was possible to construct the empirical cumulative distribution function of the uniformly transformed SPI given the uniformly transformed SPIc being lower than a certain threshold (Gimeno-Sotelo *et al* 2024b). The value that this function takes at the 5th percentile of the uniformly transformed values for the SPI is an estimation of the conditional probability of interest, i.e. $P(SPI \leqslant -1.64 | SPIc \leqslant -1.64)$.

3. Results and discussion

3.1. Sources of moisture for precipitation in regions with projected drought trends

We identified the hotspot regions where precipitation-based drought is projected to increase in a warming climate (based on the SSP5-8.5 scenario) according to the CMIP6 models used in this study. We specifically selected regions where at least 90% of the models agreed on a significant increase in the magnitude of drought events from 1850 to 2100. We found nine regions satisfying the required condition (figure 1(a)), which are consistent with the results of meteorological drought projections from previous studies (Gimeno-Sotelo *et al* 2024a, Spinoni 2020, Cook *et al* 2020, Ukkola *et al* 2020, Zhao and Dai 2022). These regions were central America (region 1), southwestern South America (region 2), northern Brazil (region 3), the Amazon (region 4), northeastern Brazil (region 5), the western Mediterranean (region 6), southern Africa (region 7), the eastern Mediterranean (region 8), and southwestern Australia (region 9).

We first analysed the main climatological moisture sources in the nine regions. The moisture sources are inextricably linked to the moisture fluxes associated with the general atmospheric circulation patterns. The picture of the seasonal vertically integrated moisture flux (figures 1(b) and (c)) gives an idea of the general pattern throughout the year, which is mainly dominated by air movement around the extended areas of high- and low-pressure centres, with important regional features such as monsoons, tropical cyclones, atmospheric rivers (ARs) and low-level jets (LLJs) (figure 1(a)). The southern branch of the subtropical high-pressure belts near 30° N and 30° S causes the trade winds to blow westward and equatorward at the Earth's surface. They merge and rise in the Intertropical Convergence Zone (ITCZ) near the equator carrying large amounts of moisture. The northern branch of the subtropical high-pressure belts flows poleward and eastward in the mid-latitudes, a movement also followed by extratropical cyclones and their associated ARs, which are the most effective systems for transporting moisture from the subtropics to the mid-latitudes, especially in winter. Seasonal differences are due to the intensification and expansion of the high-pressure belts and the poleward shift of the ITCZ during the hemispheric summer. In particular, over the northern Indian Ocean, the monsoon regime dominates the moisture flux, with moisture reaching the continent during its wet phase (northern hemisphere summer).

A schematic representation of the nine target regions (shaded in green) and their terrestrial (C1–C9) and oceanic (O1–O9) sources (shaded in orange and blue, respectively) is shown in figure 2. The moisture sources were detected using Lagrangian forward tracking during the optimal residence time of water vapour for each of the nine regions and delimited by the 90% threshold (table S1). A study region could gain moisture from more than one oceanic or terrestrial source of moisture, including its own region, through recycling processes (hereafter indicated as R). The moisture source areas detected for each region of interest are ordered in figure 2 based on the highest to lowest annual percentage contribution and are listed alphabetically. The oceanic and terrestrial sources are labelled independently. The total monthly contribution to precipitation from these specific moisture sources for each region is shown in figure 3.

For Central America (region 1), the own region acted as the most contributing moisture source (R1, 47.5%), followed by the North Atlantic source (O1A, 26%), which included the Caribbean Sea. Two oceanic sources contributed from the Pacific Ocean, with a slightly greater contribution from the North basin (10% vs. 7.9%). All the sources exhibited the same seasonal cycle (higher values during boreal summer), with a relative minimum occurring from both Pacific sources in July. Similar results were previously suggested by Durán-Quesada *et al* (2012). In

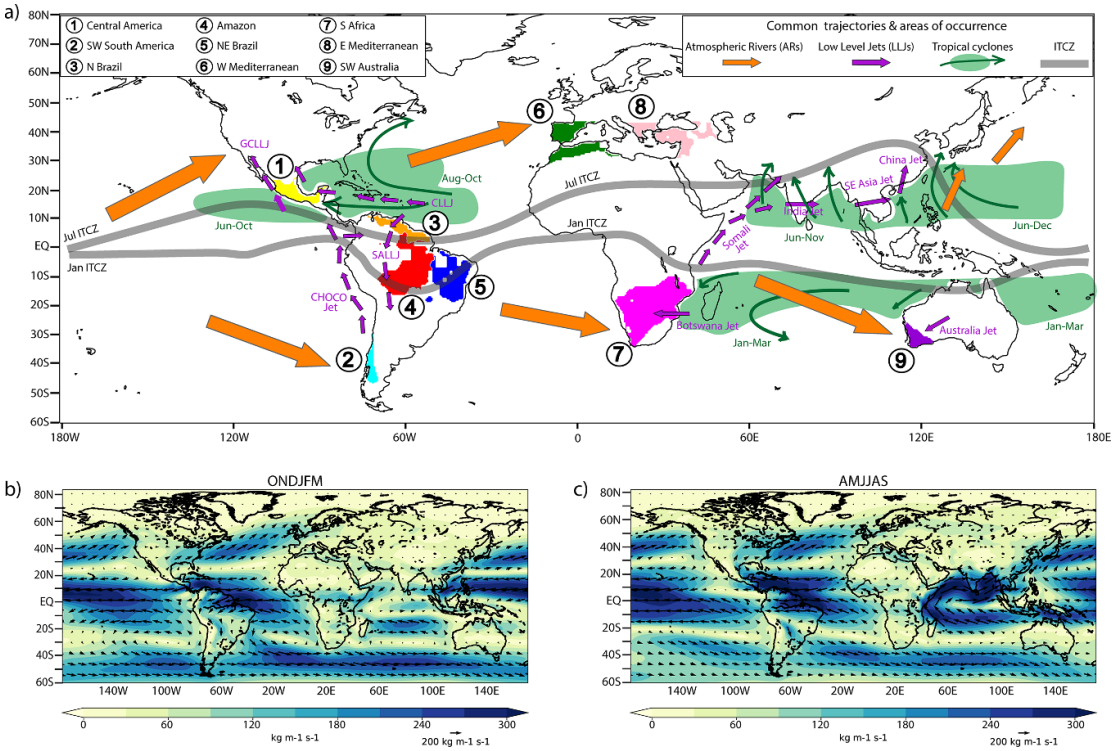

Figure 1. (a) Regions where at least 90% of the CMIP6 models used in this study agreed on a significant increase in precipitation-based drought magnitude from 1850 to 2100, together with the main moisture transport mechanisms affecting those regions (atmospheric rivers, low-level jets, and tropical cyclones). ITCZ: Intertropical Convergence Zone, GCLLJ: Gulf of California low-level jet, CLLJ: Caribbean low-level jet, SALLJ: South American low-level jet. (b), (c) Seasonally averaged vertically integrated moisture flux for October-March (ONDJFM) and April–September (AMJJAS), respectively, using ERA-Interim data for the period 1980–2018.

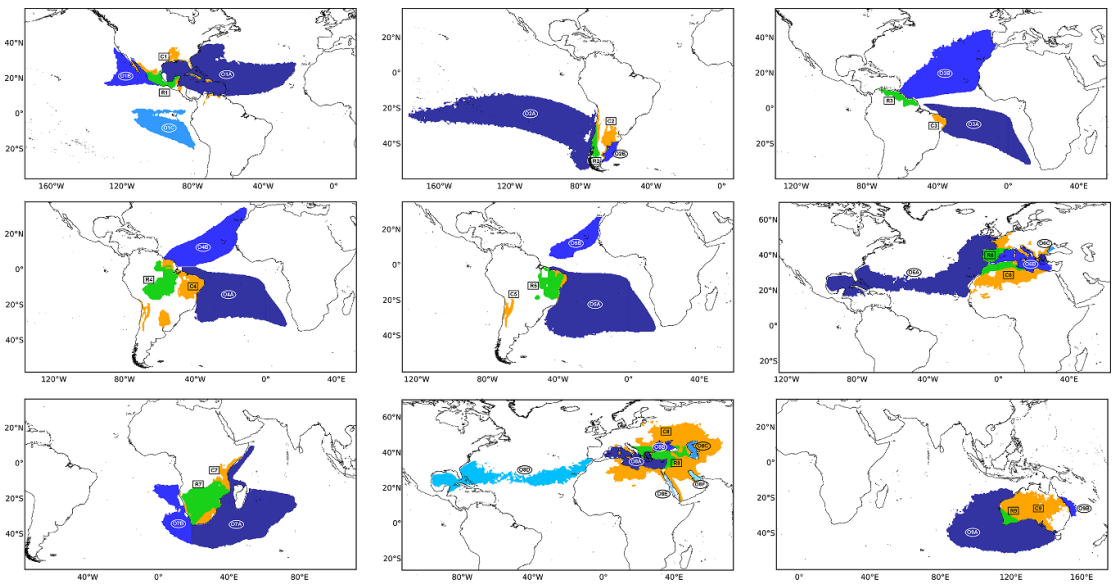

Figure 2. Schematic representation of the climatological moisture sources for the nine studied regions using ERA-Interim data: terrestrial moisture sources surrounding the region (C1–C9), the own region (R1–R9), and the different oceanic moisture source regions (the highest percentage of moisture contribution, OiA; the next, OiB; etc, where *i* is the number of the region).

general, moisture transport in the direction of central and northeastern South America is associated with the regional Caribbean LLJ from the Atlantic, the CHOCO LLJ from the South Pacific (Poveda *et al* 2014), and the Gulf of California summer coastal LLJ from the North Pacific (Parish 2000, Ordoñez *et al* 2019).

Three extratropical regions of the Southern Hemisphere were analysed: southwestern South America (region 2), southern Africa (region 7) and

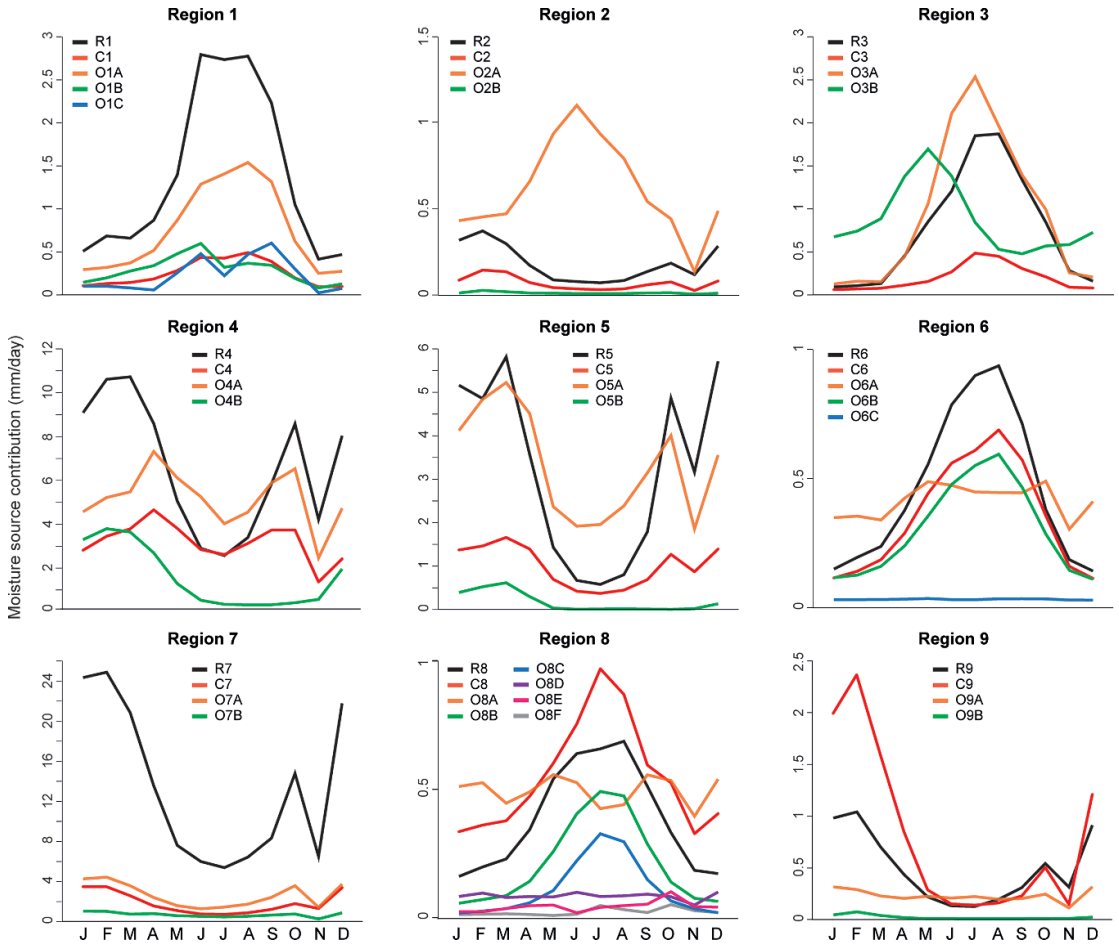

Figure 3. Monthly total contribution to precipitation from the specific moisture sources of each region for the period 1980–2018, using ERA-Interim data.

southwestern Australia (region 9). For region 2, along Chile, the most important source is the South Pacific basin (O2A, 69.8%), which supports the greatest amount of moisture throughout the year (Nieto *et al* 2014), with a marked peak in the austral winter. This maximum is linked with the ARs reaching the region (Valenzuela and Garreaud 2019, Algarra *et al* 2020) associated with extratropical cyclones, when the South Pacific high is weaker (Barret and Hameed 2017). The remaining sources, mainly the own terrestrial area (R2, 20.9%, the second source in importance) increased in relative importance, with considerable amounts occurring during the austral summer (when precipitation is often convective, Viale and Garreaud 2014) and when the South Pacific high is northwards positioned and closer to South America (Barrett and Hameed 2017). For regions 7 and 9 (southern Africa and southwestern Australia), the terrestrial sources are the most contributing ones, with R7 accounting for 72% in the former region and C9 accounting for 52.2% in the latter region. During the austral summer, high terrestrial moisture occurs due to a heat low over the interior of South Africa (Tyson and Preston-White 2000), which generates convective precipitation (Reason 2017) and is a consequence of the stronger easterlies associated with the local LLJs that inhibit moisture transport from the oceans located to their west (the Atlantic Ocean for region 7 and the Indian Ocean for region 9, Cheng and Lu 2023). The oceanic sources are spatially extensive, but they do not contribute more than 18% of the moisture to the sink regions in either case. For region 7 in winter, the Atlantic oceanic source (O7B) is associated with the passage of cyclone systems moving with westerlies and associated fronts and ARs (Reason 2017, Algarra *et al* 2020), and the Indian oceanic source (O7A) is positioned over the Agulhas Current System (Imbol Nkwinkwa *et al* 2021, Tim *et al* 2023).

For the two regions located in South America in the southern tropical band (regions 4 and 5), the main moisture source is terrestrial, with the regions themselves (R4 and R5) being the main contributors (40.35% and 41.6%, respectively), as recycling processes are relevant across these regions (Satyamurty *et al* 2013, Drumond *et al* 2019). Two oceanic moisture sources were detected for both regions, one over each basin of the Atlantic Ocean; the South Atlantic sources (O4A and O5A) provided more moisture (31.4% for region 4 and 43.1% for region 5) than did the North Atlantic sources (O4B and O5B). The

overall contribution from all these sources shows a marked seasonal cycle (see figures 1(b) and (c)), in accordance with Drumond *et al* (2019), with lower contributions occurring during June-August (austral winter, with a more easterly zonal flow) and greater contributions occurring during October–March (austral summer, when R4 and R5 support more). Region 3, positioned in the northern tropical band, is fed mainly by oceanic moisture from both Atlantic basins at a similar percentage (34.1% from the south, i.e. O3A, and 31.6% from the north, i.e. O3B), as shown by Nieto *et al* (2008) and Sorí *et al* (2023). The highest moisture contribution from its sources, except O3B, occurred during the boreal summer (Nieto *et al* 2008). These patterns of moisture transport from the Atlantic Ocean in regions 3, 4 and 5 are consistent with the easterly winds on either side of the ITCZ along the southern and northern branches of the atmospheric circulation of the North and South Atlantic subtropical high-pressure systems, respectively (Gimeno *et al* 2020, and references therein).

In the eastern façade of the North Atlantic Ocean, for regions 6 and 8, which are west and east of the Mediterranean Sea, respectively, the moisture sources contributing most are the terrestrial ones, being more important the own region for the western Mediterranean region (R6, 30.5%) and the continental surrounding areas for the eastern Mediterranean region (C8, 28.8%). The closest ocean or sea positioned west of each region is the oceanic source with the greatest contribution; that is, the North Atlantic (O6A, 27%) for region 6, and the Mediterranean Sea (O8A, 26%) for region 8. Moisture is carried by the prevailing westerly winds at these latitudes and the usual synoptic meteorological systems (cyclones and ARs). All the sources for both regions present similar seasonal behaviours, with maximum values occurring in the boreal summer and minimum values occurring in the winter. However, during summer, terrestrial sources are more important, and in winter, the major contributor is the main oceanic source. These sources and variabilities were reported in early studies (e.g. Gómez-Hernández *et al* 2013, Schicker *et al* 2010 or Batibeniz *et al* 2020).

3.2. Origin of the moisture deficit responsible for droughts

Having identified the specific moisture sources of the nine studied regions, we computed the conditional probability of drought occurrence for each region given an equivalent moisture deficit from each source using standardised indices computed at the 1 month time scale (figure 4). This time scale enables to study short-duration droughts and it is the most relevant one to unravel the influence of moisture transport deficits, considering that the typical residence time of water vapour in the atmosphere is between 3 and 10 d (Gimeno *et al* 2021). Information about the selected copula models for each region and its specific moisture sources can be found in tables S2–S10. The results showed that for five out of the eight regions, the dominant moisture source (the one for which the deficit is associated with the highest drought probability) is the specific oceanic moisture source that contributes most to precipitation in that region (regions 1, 2, 6, 8 and 9, i.e. central America, southwestern South America, the western Mediterranean, the eastern Mediterranean and southwestern Australia). For regions 4, 5 and 7 (the Amazon, northeastern Brazil and southern Africa), the dominant source is its own region and for region 3 (northern Brazil), the nearby terrestrial source is the dominant source.

In general, for all the regions where drought is dominated by specific oceanic moisture sources, our results indicate that the probability of drought occurrence given a moisture deficit from those sources is only slightly greater than that considering the dominant global moisture source (figure 2(b) in Gimeno-Sotelo *et al* 2024b). For Central America, given a moisture deficit from the dominant specific source (located in the Atlantic Ocean), the conditional probability of drought is greater than 0.30, whereas considering the dominant major moisture source in that region (the North Atlantic moisture source), the probability is between 0.10 and 0.20. For southwestern South America, for a deficit from the dominant specific source (located in the Pacific Ocean), we found a drought probability greater than 0.25, while in most of the region, considering the dominant major moisture source (South Pacific source), the probabilities are lower than that value. For the western Mediterranean, a deficit from the specific moisture source corresponding to the North Atlantic Ocean implies a drought probability close to 0.35; however, for only a small subregion in the southwestern Iberian Peninsula, the probabilities are greater than 0.25 when the dominant major moisture source (the North Atlantic) is considered. For the eastern Mediterranean, a deficit from the specific moisture source (in the Mediterranean Sea) implies a drought probability of more than 0.40 (the major moisture source, the Mediterranean Sea; in this case, it is almost coincident with the specific one, so a deficit from the major source is also associated with very high probabilities in that region). For southwestern Australia, the specific dominant moisture source is located in the Indian Ocean, and given a deficit from that source, a drought probability of more than 0.20 is found; considering the dominant general moisture source (Indian Ocean), the probability is slightly lower (between 0.10 and 0.20).

For the regions where droughts are dominated by deficits from their own region, the deficits imply very high drought probabilities in the cases of the Amazon

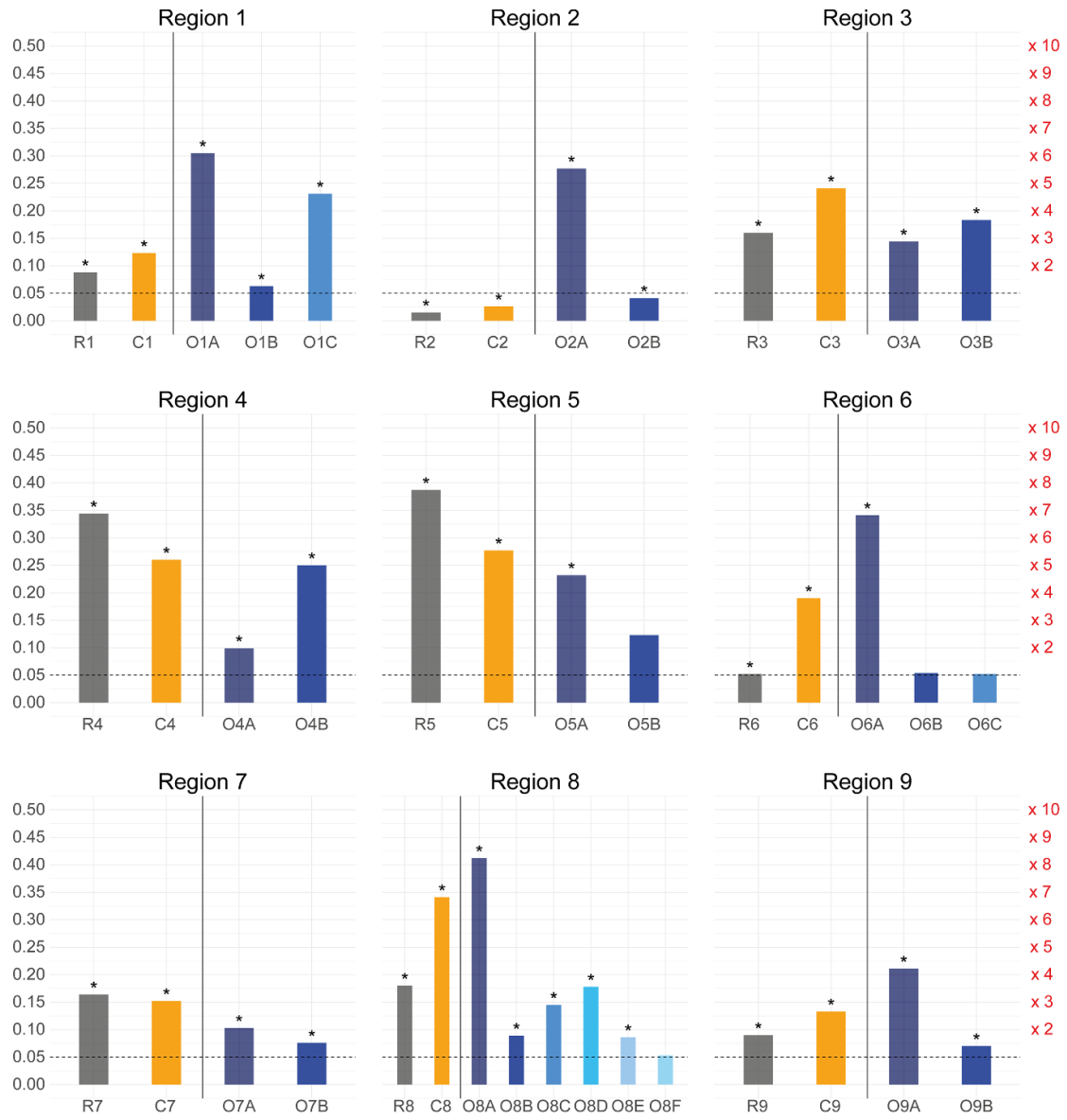

Figure 4. Conditional probability of drought occurrence given an equivalent moisture deficit from each of the specific moisture sources of each of the nine analysed regions for the standardised indices computed at the 1-month time scale. The left axis refers to the values of the probability, and the right axis indicates how many times the values are greater than the independence case (0.05). Asterisks indicate that the selected copula model fits well to the data at a significance level of 0.01.

and northeastern Brazil (close to 0.35 and close to 0.40, respectively) and a more moderate value in the case of southern Africa (slightly higher than 0.15). For northern Brazil, the deficit from the nearby terrestrial source, which is its dominant source, implies a fairly high drought probability (close to 0.25).

A relevant result is that the source that contributes the most to precipitation is not consistently the dominant source for the occurrence of droughts. Agreement occurs in four of the nine regions. In some cases, the source with the greatest contribution is the region itself for regions in areas with very strong evapotranspiration, such as the Amazon or southern Africa (region 4, region 5 and region 7). Another possibility is that the most contributing source is a remote oceanic source for a very narrow coastal area such as the Pacific coastal strip of South America (region 2).

Nonagreement takes place in five out of nine regions. This can occur when the moisture transport deficit from the oceanic source, despite not being the source contributing the most on average, is more effective in causing drought than the moisture transport deficit from the nearby continental source or the region itself (region 1, region 6, region 8 and region 9). In this case, the cascading connections between different moisture sources play a significant role. For example, there are regions where the terrestrial sources are the most contributing ones but their precipitation and enhanced moisture inputs mainly depend on remote oceanic moisture sources (figures 1(b) and (c) for a general view of the atmospheric circulation, which influences moisture transport; Gimeno *et al* 2012 for a review on the link moisture sources-sinks; and Gimeno *et al* 2016 for

moisture transport mechanisms). A low contribution from the terrestrial sources (either the own region or the nearby continental source) does not necessarily imply a low contribution from the remote oceanic sources. However, and given cascading effects, a low contribution from the remote oceanic sources would imply a low contribution from the terrestrial sources with a greater or lesser delay as moisture availability decreases. This cascading effect is possible even on the one-month timescale used to analyse droughts, because moisture transport has a timescale linked to the residence time of water vapour in the atmosphere, typically between 3 and 10 d (Gimeno *et al* 2021), which is shorter than the timescale used in this article and therefore allows cascading effects. The difference between target regions where the most contributing terrestrial source dominates drought occurrence (regions 4, 5, and 7, mostly tropical) and target regions where the most contributing terrestrial source does not dominate (regions 1, 6, 8 and 9, mostly extratropical) would be explained by the fact that land evapotranspiration is more intense in tropical humid regions due to high atmospheric evaporative demand, so that recycling processes would dominate drought occurrence in the short term (Wang and Dickinson 2012, Singer *et al* 2021). All these processes, which are characterised by strong spatial variability, would explain why the deficit in the moisture contribution from oceanic moisture sources takes longer to produce a deficit in the contribution from the terrestrial sources of regions in tropical humid areas than in extratropical ones. For example, the probability that the contribution from the most contributing terrestrial source is lower than its 5% percentile, conditional on the contribution from the most contributing oceanic one being lower than its 5% percentile, is only 0.10 for region 4 (the Amazon), while it is as high as 0.39 for region 6 (western Mediterranean), i.e. almost four times higher. It is explained by the higher evapotranspiration values in the former (a tropical region) than in the latter one (an extratropical region). Thus, in extratropical target regions, a deficit in the contribution from distant oceanic sources has a more direct impact on drought occurrence than in tropical target regions. Nonagreement may also occur when the dominant source for drought occurrence is placed in the path of the moisture transported from both the most contributing remote oceanic source and another secondary remote oceanic source (region 3).

Although the results reported in this study refer to the present climate and source extents and intensities and drought probability values may vary in the future, they are highly relevant regarding climate change implications. The dominant moisture sources of regions 1, 2, 6, 8 and 9, which are oceanic, and the one corresponding to region 4, which is terrestrial (its own region) are located in areas where the balance between evaporation and precipitation is projected to increase strongly according to CMIP6 climate models (figure 5 in Allan 2023). Furthermore, a large proportion of the dominant sources are located in areas that are likely to experience changes in atmospheric circulation (Allan *et al* 2020), such as the narrowing and intensification of the ITCZ (which would affect the dominant source of regions such as 3 or 4) or the expansion to higher latitudes of the storm track and associated moisture transport mechanisms such as ARs (which would affect the dominant source of regions such as 1, 2, 6 and 8).

4. Concluding remarks

In this paper, we focused on regions for which climate models show the greatest agreement in increases in drought magnitude in the future climate. We identified the main climatological moisture sources of these regions and analysed the influence of moisture transport deficits from these sources on drought occurrence in the regions. We reached three important conclusions:

For the nine identified regions, there are a variety of situations for the dominant sources for drought; with three regions where it is the region itself (the Amazon, northeastern Brazil and southern Africa), highlighting the role of recycling; one region where it is the nearby terrestrial source (northern Brazil), and five regions where it is an oceanic source (central America, southwestern South America, both western and eastern Mediterranean and southwestern Australia).

The probability of drought occurrence given an equivalent contribution deficit from the dominant specific moisture source of a given region is generally high. In some cases, the drought probability is as high as 0.40, a value that is eight times greater than the one corresponding to the independence case (i.e. in which contribution deficit and drought are unrelated). However, in general, considering the moisture deficit from specific moisture sources instead of the deficit from major global moisture sources (Gimeno-Sotelo *et al* 2024b) provides only slightly higher drought probabilities.

The source that dominates drought occurrence in a region, i.e. the one associated with the highest probability, does not consistently coincide with the source that contributes the most to the precipitation in each region. This should be understood in terms of the cascading connections between different moisture sources, which explain why, in some regions, droughts predominantly depend on oceanic moisture sources despite the fact that the terrestrial sources are the most contributing ones. In those cases, low contributions from the oceanic sources imply low contributions from the terrestrial ones, especially in extratropical target regions, where land evapotranspiration is

less intense than in tropical humid ones. This result is especially remarkable when contextualising the importance of the results, since we should focus on what will happen in these dominant moisture sources to correctly interpret how moisture transport deficits affect droughts at the regional scale. It should be noted that we analysed the moisture sources and their importance in drought occurrence in the present climate and did not evaluate how these sources may vary in the future, which would undoubtedly merit future studies.

Data availability statement

The data that support the findings of this study are openly available at the following URLs: https://esgf-node.llnl.gov/search/cmip6/; www.flexpart.eu/downloads; www.gloh2o.org/mswep/.

Acknowledgments

EPhysLab members are supported by the PID2021-122314OB-I00 and TED2021-129152B-C41/TED2021-129152B-C43 projects funded by the Ministerio de Ciencia, Innovación y Universidades, Spain (MICIU/AEI/10.13039/501100011033), Xunta de Galicia under the Project ED431C2021/44 (Programa de Consolidación e Estructuración de Unidades de Investigación Competitivas (Grupos de Referencia Competitiva) and Consellería de Cultura, Educación e Universidade), and by the European Union 'ERDF A way of making Europe' 'NextGenerationEU'/PRTR. Luis Gimeno-Sotelo was supported by a 'Ministerio de Ciencia,Innovación y Universidades' PhD Grant (reference: PRE2022-101497). Milica Stojanovic acknowledges the Grant No. ED481B-2021/134 from the Xunta of Galicia (regional government), and Rogert Sorí the grant RYC2021-034044-I funded by Ministerio de Ciencia, Innovación y Universidades, Spain (MICIU/ AEI/10.13039/501100011033) and the European Union Next Generation EU/PRTR. This work has also been possible thanks to the computing resources and technical support provided by CESGA (Centro de Supercomputación de Galicia) and RES (Red Española de Supercomputación). This study was also supported by the 'Unidad Asociada CSIC–Universidade de Vigo: Grupo de Física de la Atmósfera y del Océano'.

Author contributions

Luis Gimeno-Sotelo designed the experiments and contributed to data analysis and paper writing. Milica Stojanovic and Rogert Sorí performed the Lagrangian analysis and contributed to paper writing. Raquel Nieto contributed to the creation of the final figures and paper writing. Sergio M Vicente-Serrano contributed to the discussion of the results. Luis Gimeno conceived the idea for the study and contributed to the writing of the paper. All the authors contributed to the review and editing of the manuscript.

ORCID iDs

Luis Gimeno-Sotelo https://orcid.org/0000-0001-9305-2325
Milica Stojanovic https://orcid.org/0000-0002-6783-9025
Luis Gimeno https://orcid.org/0000-0002-0778-3605

References

Akaike H 1974 A new look at the statistical model identification *IEEE Trans. Autom. Control* **19** 716–23
Algarra I, Nieto R, Ramos A M, Eiras-Barca J, Trigo R M and Gimeno L 2020 Significant increase of global anomalous moisture uptake feeding landfalling atmospheric rivers *Nat. Commun.* **11** 5082
Allan R P *et al* 2020 Advances in understanding large-scale responses of the water cycle to climate change *Ann. New York Acad. Sci.* **1472** 49–75
Allan R P 2023 Amplified seasonal range in precipitation minus evaporation *Environ. Res. Lett.* **18** 094004
Bachmair S, Kohn I and Stahl K 2015 Exploring the link between drought indicators and impacts *Nat. Hazards Earth Syst. Sci.* **15** 1381–97
Barrett B S and Hameed S 2017 Seasonal variability in precipitation in Central and Southern Chile: modulation by the South Pacific high *J. Clim.* **30** 55–69
Batibeniz F, Ashfaq M, Önol B, Turuncoglu U U, Mehmood S and Evans K J 2020 Identification of major moisture sources across the Mediterranean Basin *Clim. Dyn.* **54** 4109–27
Beck H E, van Dijk A I J M, Levizzani V, Schellekens J, Miralles D G, Martens B and de Roo A 2017 MSWEP: 3-hourly 0.25° global gridded precipitation (1979–2015) by merging gauge, satellite, and reanalysis data *Hydrol. Earth Syst. Sci.* **21** 589–615
Cammalleri C *et al* 2020 *Global warming and drought impacts in the EU* (Publications Office of the European Union) (https://doi.org/10.1016/j.ejrh.2020.100723)
Cheng T F and Lu M 2023 Global Lagrangian tracking of continental precipitation recycling, footprints, and cascades *J. Clim.* **36** 1923–41
Cook B I, Mankin J S, Marvel K, Williams A P, Smerdon J E and Anchukaitis K J 2020 Twenty-first century drought projections in the CMIP6 forcing scenarios *Earth's Future* **8** e2019EF001461
Czado C 2019 *Analyzing Dependent Data with Vine Copulas (Lecture Notes in Statistics)* (Springer) p 222
Dee D P *et al* 2011 The ERA-Interim reanalysis: configuration and performance of the data assimilation system *Q. J. R. Meteorol. Soc.* **137** 553–97
Douville H *et al* 2021 Water cycle changes *Climate Change 2021: The Physical Science Basis. Contribution of Working Group I to the Sixth Assessment Report of the Intergovernmental Panel on Climate Change* ed V Masson-Delmotte (Cambridge University Press) pp 1055–210
Drumond A, Stojanovic M, Nieto R, Vicente-Serrano S M and Gimeno L 2019 Linking anomalous moisture transport and drought episodes in the IPCC reference regions *Bull. Am. Meteorol. Soc.* **100** 1481–98
Durán-Quesada A M, Reboita M and Gimeno L 2012 Precipitation in tropical America and the associated sources of moisture: a short review *Hydrol. Sci. J.* **57** 612–24

Erian W, Pulwarty R, Vogt J V, AbuZeid K, Bert F, Bruntrup M and Zougmore R B 2021 *GAR special report on drought 2021* (United Nations Office for Disaster Risk Reduction (UNDRR))

Eyring V, Bony S, Meehl G A, Senior C A, Stevens B, Stouffer R J and Taylor K E 2016 Overview of the coupled model intercomparison project phase 6 (CMIP6) experimental design and organization *Geosci. Model Dev.* **9** 1937–58

Fernández-Álvarez J C, Pérez-Alarcón A, Eiras-Barca J, Rahimi S, Nieto R and Gimeno L 2023 Projected changes in atmospheric moisture transport contributions associated with climate warming in the North Atlantic *Nat. Commun.* **14** 6476

Fernández-Alvarez J C, Vázquez M, Pérez-Alarcón A, Nieto R and Gimeno L 2023 Comparison of moisture sources and sinks estimated with different versions of FLEXPART and FLEXPART-WRF models forced with ECMWF reanalysis data *J. Hydrometeorol.* **24** 221–39

Fleig A K, Tallaksen L M, Hisdal H and Demuth S 2006 A global evaluation of streamflow drought characteristics *Hydrol. Earth Syst. Sci.* **10** 535–52

Garcia-Herrera R, Garrido-Perez J M, Barriopedro D, Ordóñez C, Vicente-Serrano S M, Nieto R, Gimeno L, Sorí R and Yiou P 2019 The European 2016/2017 drought *J. Clim.* **32** 3169–87

Gimeno L, Dominguez F, Nieto R, Trigo R, Drumond A, Reason C J, Taschetto A S, Ramos A M, Kumar R and Marengo J 2016 Major mechanisms of atmospheric moisture transport and their role in extreme precipitation events *Annu. Rev. Environ. Resour.* **41** 117–41

Gimeno L, Drumond A, Nieto R, Trigo R M and Stohl A 2010a On the origin of continental precipitation *Geophys. Res. Lett.* **37** L13804

Gimeno L, Eiras-Barca J, Durán-Quesada A M, Dominguez F, van der Ent R, Sodemann H, Sánchez-Murillo R, Nieto R and Kirchner J W 2021 The residence time of water vapour in the atmosphere *Nat. Rev. Earth Environ.* **2** 558–69

Gimeno L, Nieto R, Trigo R M, Vicente S and Lopez-Moreno J I 2010b Where does the Iberian Peninsula moisture come from? An answer based on a Lagrangian approach *J. Hydrometeorol.* **11** 421–36

Gimeno L, Stohl A, Trigo R M, Domínguez F, Yoshimura K, Yu L, Drumond A, Durán-Quesada A M and Nieto R 2012 Oceanic and terrestrial sources of continental precipitation *Rev. Geophys.* **50** RG4003

Gimeno L, Vázquez M, Eiras-Barca J, Sorí R, Stojanovic M, Algarra I, Nieto R, Ramos A M, Durán-Quesada A M and Dominguez F 2020 Recent progress on the sources of continental precipitation as revealed by moisture transport analysis *Earth Sci. Rev.* **201** 103070

Gimeno-Sotelo L, Sorí R, Nieto R, Vicente-Serrano S M and Gimeno L 2024b Unravelling the origin of the atmospheric moisture deficit that leads to droughts *Nat. Water* **2** 242–53

Gimeno-Sotelo L *et al* 2024a Assessment of the global relationship of different types of droughts in model simulations under high anthropogenic emissions *Earth's Future* **12** e2023EF003629

Gómez-Hernández M, Drumond A, Gimeno L and Garcia-Herrera R 2013 Variability of moisture sources in the Mediterranean region during the period 1980–2000 *Water Resour. Res.* **49** 6781–94

Herrera-Estrada J E, Martinez J A, Dominguez F, Findell K L, Wood E F and Sheffield J 2019 Reduced moisture transport linked to drought propagation across North America *Geophys. Res. Lett.* **46** 5243–53

Hersbach H *et al* 2020 The ERA5 global reanalysis *Q. J. R. Meteorol. Soc.* **146** 1999–2049

Holgate C M, Van Dijk A I J M, Evans J P and Pitman A J 2020 Local and remote drivers of southeast Australian drought *Geophys. Res. Lett.* **47** e2020GL090238

Huang W and Prokhorov A 2014 A goodness-of-fit test for copulas *Econ. Rev.* **33** 751–71

Imbol Nkwinkwa A S N, Rouault M, Keenlyside N and Koseki S 2021 Impact of the Agulhas current on Southern Africa precipitation: a modeling study *J. Clim.* **34** 9973–88

IPCC 2022 Climate change 2022: impacts, adaptation and vulnerability *Contribution of Working Group II to the Sixth Assessment Report of the Intergovernmental Panel on Climate Change* ed H-O Pörtner *et al* (Cambridge University Press) p 3056

Kendall M G 1948 Rank correlation methods

Mann H B 1945 Nonparametric tests against trend *Econometrica* **13** 245–59

McKee T B, Doesken N J and Kleist J 1993 The relationship of drought frequency and duration to time scales *Proc. 8th Conf. on Applied Climatology* vol 17 pp 179–83

Naumann G, Camalleri C, Mentaschi L and Feyen L 2021 Increased economic drought impacts in Europe with anthropogenic warming *Nat. Clim. Change* **11** 485–91

Nieto R, Castillo R, Drumond A and Gimeno L 2014 A catalog of moisture sources for continental climatic regions *Water Resour. Res.* **50** 5322–8

Nieto R, Gallego D, Trigo R, Ribera P and Gimeno L 2008 Dynamic identification of moisture sources in the Orinoco basin in equatorial South America *Hydrol. Sci. J.* **53** 602–17

Nieto R and Gimeno L 2019 A database of optimal integration times for Lagrangian studies of atmospheric moisture sources and sinks *Sci. Data* **6** 59

Nieto R and Gimeno L 2021 Addendum: a database of optimal integration times for Lagrangian studies of atmospheric moisture sources and sinks *Sci. Data* **8** 130

NOAA-NCEI (National Oceanic and Atmospheric Administration National Centers for Environmental Information) 2021 U.S. billion-dollar weather and climate disasters: overview (available at: www.ncdc.noaa.gov/billions/)

Ordoñez P, Nieto R, Gimeno L, Ribera P, Gallego D, Ochoa-Moya C A and Quintanar A I 2019 Climatological moisture sources for the Western North American Monsoon through a Lagrangian approach: their influence on precipitation intensity *Earth Syst. Dyn.* **10** 59–72

Parish T R 2000 Forcing of the summertime low-level jet along the California coast *J. Appl. Meteorol.* **39** 2421–33

Pisso I *et al* 2019 The Lagrangian particle dispersion model FLEXPART version 10.4 *Geosci. Model Dev.* **12** 4955–97

Poveda G, Jaramillo L and Vallejo L F 2014 Seasonal precipitation patterns along pathways of South American low-level jets and aerial rivers *Water Resour. Res.* **50** 98–118

Reason C J C 2017 Climate of southern Africa *Oxford Research Encyclopedia of Climate Science* p 450

Roy T, Martinez J A, Herrera-Estrada J E, Zhang Y, Dominguez F, Berg A, Ek M and Wood E F 2019 Role of moisture transport and recycling in characterizing droughts: perspectives from two recent U.S. droughts and the CFSv2 system *J. Hydrometeorol.* **20** 139–54

Salah Z, Nieto R, Drumond A, Gimeno L and Vicente-Serrano S 2018 A Lagrangian analysis of the moisture budget over the fertile crescent during two intense drought episodes *J. Hydrol.* **560** 382–95

Satyamurty P, da Costa C P W and Manzi A O 2013 Moisture source for the Amazon Basin: a study of contrasting years *Theor. Appl. Climatol.* **111** 195–209

Schicker I, Radanovics S and Seibert P 2010 Origin and transport of Mediterranean moisture and air *Atmos. Chem. Phys.* **10** 5089–105

Schumacher D L, Keune J, Dirmeyer P and Miralles D G 2022 Drought self-propagation in drylands due to land–atmosphere feedbacks *Nat. Geosci.* **15** 262–8

Seneviratne S I *et al* 2021 Weather and climate extreme events in a changing climate *Climate Change 2021: The Physical Science Basis. Contribution of Working Group I to the Sixth Assessment Report of the Intergovernmental Panel on Climate Change V* Masson-Delmotte ed (Cambridge University Press) pp 1513–766

Singer M B, Asfaw D T, Rosolem R, Cuthbert M O, Miralles D G, MacLeod D, Quichimbo E A and Michaelides K 2021

Hourly potential evapotranspiration at 0.1° resolution for the global land surface from 1981-present *Sci. Data* **8** 224

Sorí R, Gimeno-Sotelo L, Nieto R, Liberato M L, Stojanovic M, Pérez-Alarcón A, Gimeno L and Gimeno L 2023 Oceanic and terrestrial origin of precipitation over 50 major world river basins: implications for the occurrence of drought *Sci. Total Environ.* **859** 160288

Spinoni J *et al* 2020 Future global meteorological drought hot spots: a study based on CORDEX data *J. Clim.* **33** 3635–61

Stine S 1994 Extreme and persistent drought in California and Patagonia during mediaeval time *Nature* **369** 546–9

Stohl A, Forster C, Frank A, Seibert P and Wotawa G 2005 The Lagrangian particle dispersion model FLEXPART version 6.2 *Atmos. Chem. Phys.* **5** 2461–74

Tallaksen L M, Madsen H and Clausen B 1997 On the definition and modelling of streamflow drought duration and deficit volume *Hydrol. Sci. J.* **42** 15–33

Tim N, Zorita E, Hünicke B and Ivanciu I 2023 The impact of the Agulhas current system on precipitation in Southern Africa in regional climate simulations covering the recent past and future *Weather Clim. Dyn.* **4** 381–97

Trenberth K E, Dai A, Rasmussen R M and Parsons D B 2003 The changing character of precipitation *Bull. Am. Meteorol. Soc.* **84** 1205–18

Tyson D and Preston-White R A 2000 *The Weather and Climate of Southern Africa* (Oxford University Press)

Ukkola A, De Kauwe M, Roderick M, Abramowitz G and Pitman A J 2020 Robust future changes in meteorological drought in CMIP6 projections despite uncertainty in precipitation *Geophys. Res. Lett.* **47** e2020GL087820

Valenzuela R A and Garreaud R D 2019 Extreme daily rainfall in central-southern Chile and its relationship with low-level horizontal water vapor fluxes *J. Hydrometeorol.* **20** 1829–50

Vázquez M, Nieto R, Liberato M L R and Gimeno L 2020 Atmospheric moisture sources associated with extreme precipitation during the peak precipitation month *Weather Clim. Extremes* **30** 100289

Viale M and Garreaud R 2014 Summer precipitation events over the western slope of the subtropical Andes *Mon. Weather Rev.* **142** 1074–92

Wang K and Dickinson R E 2012 A review of global terrestrial evapotranspiration: observation, modeling, climatology, and climatic variability *Rev. Geophys.* **50** RG2005

Wei J and Dirmeyer P A 2019 Sensitivity of land precipitation to surface evapotranspiration: a nonlocal perspective based on water vapor transport *Geophys. Res. Lett.* **46** 12588–97

White H 1982 Maximum likelihood estimation of misspecified models *Econometrica* **50** 1–25

Wilhite D A, Svoboda M D and Hayes M J 2007 Understanding the complex impacts of drought: a key to enhancing drought mitigation and preparedness *Water Resour. Manage.* **21** 763–74

World Meteorological Organization. Standardized Precipitation Index User Guide 2012 (available at: https://library.wmo.int/records/item/39629-standardized-precipitation-index-user-guide)

Woxodhouse C A, Meko D M, MacDonald G M, Stahle D W and Cook E R 2010 A 1,200-year perspective of 21st century drought in Southwester North America *Proc. Natl Acad. Sci. USA* **107** 21283–8

Zhao T and Dai A 2022 CMIP6 model-projected hydroclimatic and drought changes and their causes in the twenty-first century *J. Clim.* **35** 897–921